Article

Fe-Assisted Synthesis of Si Nanowires

Iftikhar Ahmad, Michael Fay, Yongde Xia, Xianghui Hou, Andrew Kennedy, and Yanqiu Zhu

J. Phys. Chem. C, **2009**, 113 (4), 1286-1292• DOI: 10.1021/jp808492t • Publication Date (Web): 07 January 2009

Fe-Assisted Synthesis of Si Nanowires

Iftikhar Ahmad,[†] Michael Fay,[‡] Yongde Xia,[†] Xianghui Hou,[†] Andrew Kennedy,[†] and Yanqiu Zhu*[,†,‡]

School of Mechanical, Materials and Manufacturing Engineering, The University of Nottingham, University Park, Nottingham, NG7 2RD, United Kingdom, and Nottingham NanoScience and NanoTechnology Centre (NNNC), The University of Nottingham, University Park, Nottingham NG7 2RD, United Kingdom

Received: September 24, 2008; Revised Manuscript Received: October 31, 2008

Ultrafine and pure Si-nanowires (SiNWs) have been synthesized with the assistance of carbon nanotubes (CNTs) during a chemical vapor deposition process via the vapor liquid solid (VLS) mechanism. A mixture of CNTs and Si_3N_4 produces a high yield of fine SiNWs upon heating at 1600 °C under Ar atmosphere. Fe nanoparticles, located at the tip of CNTs, have been employed as a catalyst for the growth of nanowires and carbon acted as a reducing agent during the synthesis process. The resulting SiNWs have been appraised by SEM, TEM, XRD, Raman, BET, and FTIR to investigate the morphology, structure, and surface characteristics. Electron microscopic studies have demonstrated that the SiNWs have a uniform diameter of 7−17 nm, being single crystalline and enveloped with a tiny sheath of SiO_x ($x = 1\sim2$). Furthermore, hydrofluoric acid etching can remove the oxide shell, leading to much purer and finer SiNWs. Nitrogen-sorption isotherms indicate that SiNWs have very high BET specific surface areas. The high yield, ultrafine size, and large surface areas cumulatively offer these nanowires a great potential as candidates for advanced applications in nanodevices, fuel cells, and catalysis.

1. Introduction

The revolutionary discovery of CNTs has a significant impact on nanomaterials research and nanotechnologies.[1] On the one hand, these tiny nanotubes are an excellent candidate for direct nanodevice constructions, such as in field emission probe, gas storage, super capacitors, and as a reinforcement for composite materials. On the other hand, they can be used indirectly as templates for the synthesis of other novel nanostructures, such as SiNWs, SiC and Si_3N_4 nanorods, SiC carbide nanowires, and SiC coaxial nanocables by laser ablation or by high-temperature carbothermal reduction of silica xerogels.[2] As the most important semiconducting material, SiNWs exhibited many exceptional properties in electronic, optical, and chemical applications and they are considered to be one of the most promising candidates for future application in a nanodevice.[3] So far, SiNWs have been prepared by employing different techniques, such as laser ablation, physical thermal evaporation, chemical vapor deposition, and other methods.[4−9] Si nanostructures are often sheathed with an amorphous silicon oxide layer and it has been reported that this shell is responsible for the decrease of the chemical sensitivity of SiNWs to the NH_3 gas and water vapors.[10] SiNWs have abundant defects such as microtwins and stacking faults, which also influence the future applications. After decades of effort, VLS growth becomes a well-defined mechanism for the growth of crystalline wirelike structures during which a liquid metal cluster or catalyst, generally Au, acts as the energetically favored site for absorption of the gas-phase reactant.[11] Therefore, the controlled growth of 1D structure is somehow limited by the minimum available diameters of the liquid-metal catalyst that can be achieved under equilibrium conditions.[12] Other than the VLS method, Buhro has reported the solution-liquid solid (SLS) synthesis of SiNWs with diameters ranging from 10−100 nm.[13] Most recently, single-crystal SiNWs with the prism structure were generated with the assistance of CNTs by CVD deposition of a volatile SiH_4 gas at 450 °C and Fe catalyst from the CNTs played an important part during the crystalline growth of SiNWs with diameters of 50−70 nm.[14] SiNWs were also produced by reacting silicon powder or silicon substrate with carbon in an inert atmosphere at 1200−1350 °C.[15] However, the diameters of the resulting SiNWs were rather large, between 75−350 nm. To date, available studies seem to suggest that the chemically synthesized SiNWs have a large and uneven diameter distribution; in particular the yield is not sufficient to meet the large quantity requirement of practical industry applications. In this report, we demonstrate a CVD synthesis of the ultrafine, uniform, and single-crystalline SiNWs in high yield with the assistance of unpurified CNTs. To verify the actual catalytic role of CNTs, pure Fe_2O_3 nanoparticles were also used as a catalyst for comparison, resulting in similar nanowires. This study will offer enhanced potentials for advanced applications of SiNWs with finer diameters.

2. Experimental Section

Si_3N_4 (∅ 25 nm, Sigma Aldrich, UK) with a minute amount of additives (MgO and Y_2O_3) along with 5 wt % CNTs (∅ ∼ 40 nm, Tsinghua University, China) were mixed using an ultrasonic probe in acetone. After drying, the powder mixture was milled and placed at the center of an Al_2O_3 working tube inside a horizontal tube furnace. High-purity argon was used as a carrier gas flowing through the pre-evacuated Al_2O_3 tube at a rate of 300 mL/min. The heating time was 60 min at 1600 °C. Parallel process was carried out using 5 wt % Fe_2O_3 nanoparticles (∅ 20−40 nm) instead of CNTs for comparison. In both cases, after heating a large amount of brown sponge material was collected from the Al_2O_3 working tube, which was carefully processed and appraised by SEM (Philips/FEI XL30-

* To whom correspondence should be addressed. E-mail: Yanqiu.Zhu@nottingham.ac.uk.
† School of Mechanical, Materials and Manufacturing Engineering.
‡ Nottingham NanoScience and NanoTechnology Centre (NNNC).

10.1021/jp808492t CCC: $40.75
Published on Web 01/07/2009

JEOL 6400, Philips/FEI XL30 FEG-ESEM) and images were acquired by using secondary electron (SE) signals and attached EDX was used for quantitative elemental analysis of SiNWs. X-ray diffraction of Cu kα radiation was applied (Siemens D500 and Bruker D8 Advanced X-ray Differactometer) to identify the crystalline-phase structures. The acquired peaks were analyzed by using computer software *DIFFRAC*^{plus} Release 2004, by Bruker Advanced X-ray Solutions. TEM (JEOL 2000 FX and 2100 F) were used for qualitative investigations of the SiNWs, samples were prepared by dispersing the SiNWs in acetone and then transferred onto a holey carbon film supported on a copper grid, and attached EDX (Oxford Instrument IncaEnergy, UK) was used for quantitative analysis of the compositional feature of the nanowires and the catalyst. To analyze SiNWs size distribution, 100 nanowires were randomly selected from the TEM images acquired from different locations and diameters of individual nanowires were obtained using computer software *ImageJ* (Image Processing and Analysis in Java).

A fourier transformation infrared (FTIR) spectrometer was carried out by employing a Bruker Tensor-27 FTIR. The spectral resolution in the experiment was 0.5 cm^{-1} in the range of 500−2000 cm^{-1}. Raman spectroscopy was carried out with *LabRAM* from Horiba Jobin Yvon Ltd., with a HeNe laser at a wavelength of 633 nm. The as-prepared SiNWs were etched with a 20% hydrofluoric acid (HF) for 30 min and then rinsed with distilled water to remove residual acid. Nitrogen-sorption isotherms and textural properties of both synthesized and etched SiNWs were determined at −196 °C using nitrogen in a conventional volumetric technique by a Micromeritics ASAP2020 sorptometer. Before analysis, the samples were oven-dried at 250 °C and evacuated for 12 h. The surface area was calculated using the BET (Brunauer−Emmett−Teller) method based on adsorption data in the partial pressure (P/P_o) range 0.05 to 0.2, and total pore volume was determined from the amount of the nitrogen adsorbed at $P/P_o = 0.99$.

3. Results and Discussion

3.1. Structural Characterization. Yellowish/brownish material was produced during the reaction in high yield (20 wt % of the precursor), and about 1 g SiNWs was collected in each run, as shown in part A of Figure 1. CNTs employed for SiNWs growth are displayed in part B of Figure 1 with Fe catalyst in the inset and XRD examination of CNTs, parts C and a of Figure 1, revealed graphite peak (JCPDS No. 01−075−1621). The XRD pattern of the SiNWs exhibited strong and sharp peaks of a cubic Si phase (JCPDS No. 27−1402), along with minor peaks that can be attributed to the surface SiO_x (JCPDS No. 42−1401), intensities b and c of part C of Figure 1. Upon exposure in air, a prominent surface oxidation layer is generally present on SiNWs due to their high surface-to-volume ratio.[15] After HF-etching, the SiNWs exhibited highly crystalline features of pure Si, in intensity d of part C Figure 1, because HF has removed the surface amorphous layer of the SiNWs, to produce rather pure nanowires.

Numerous entangled nanowires were observed by using SEM for the as-prepared materials, part a of Figure 2. On close inspection, parts b and c of Figure 2 exhibited fairly uniform nanowires, with diameters dominantly in the range of ∼7−17 nm and several micrometers in length. The SiNWs synthesized using Fe_2O_3 nanoparticles are shown in parts d and e of Figure 2, which reveal the nonuniform diameters. EDX analysis of a single nanowire confirms that it contains only Si and O, as demonstrated in part f of Figure 2.

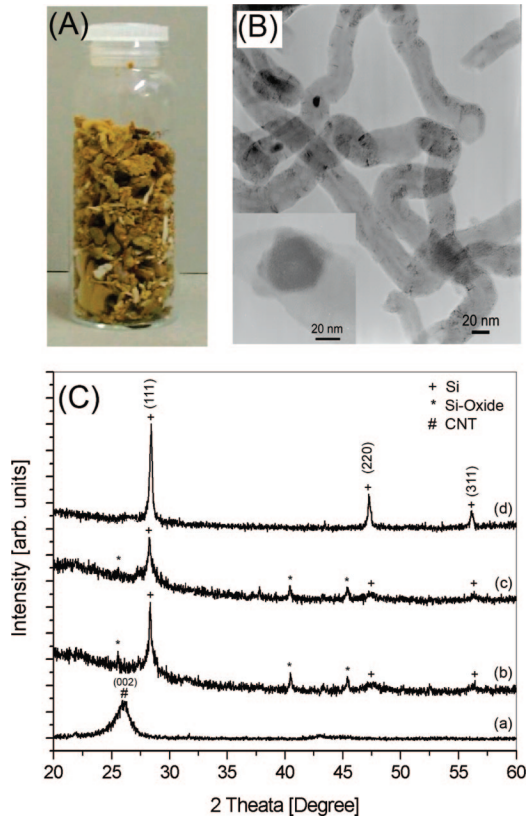

Figure 1. (A) As synthesis SiNWs, (B) CNTs with Fe catalyst in inset, (C) XRD pattern of CNTs (a); SiNWs produced with Fe-containing CNTs (b); catalyzed directly by Fe_2O_3 nanoparticles (c); and the HF-etched SiNWs (d).

In Figure 3, the TEM investigations of CNTs-assisted SiNWs again revealed the uniform diameters, however nonuniform SiNWs were also apparent for the Fe_2O_3-catalyzed nanowires. The HF-etched SiNWs are shown in part c of Figure 3, which clearly retained their original 1D shape. HRTEM images recorded on individual nanowires, part d of Figure 3, provide further insight into the structure of these nanowires, which consist of a single-crystal metal catalyst, the single-crystal SiNWs, and the amorphous SiO_x shell. The uniform crystalline core is 6−8 nm, surrounded by an amorphous SiO_x layer of thickness >5 nm. A selected area diffraction pattern illustrates that the crystalline Si core growth occurs along the [211] direction, which was confirmed in the lattice resolved TEM images, as seen in part f of Figure 3. It is clearly shown that the (111) atomic planes with a 0.31 nm separation have a sharp interface with the amorphous SiO_x. The amorphous oxide shell of SiO_x was successfully removed or reduced by etching with HF, and part f of Figure 3 exhibits a minute SiO_x layer thinner than 2 nm as compared to the unetched nanowire (>5 nm). EDX analysis of a single SiNW tip detected Fe and Si during TEM investigation, part c of Figure 4, and the nanowire body exhibited only Si and O, as shown in part b of Figure 4.

3.2. Spectral Features and Adsorption Properties. FTIR absorption spectroscopy is used to investigate the structural and compositional properties of certain oxides and the absorption band of SiNWs is normally cantered at 1000−1130 cm^{-1}.[16] Part a of Figure 5 indicates that the absorption bands in our case fall in the same range with the strongest absorption peaks centered at 1042 and 1068 cm^{-1} for the as-prepared and the HF-etched SiNWs, respectively. The etched SiNWs absorption peak appeared at slightly higher frequency may be associated with the thin SiO_x shell around the SiNWs crystalline core. The

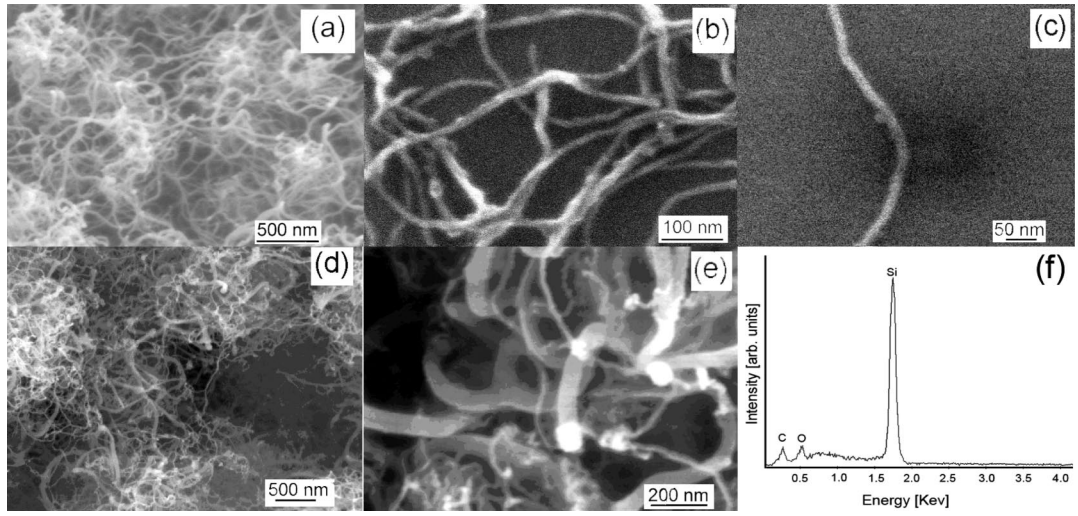

Figure 2. SEM images of SiNWs synthesized with CNTs (a−c), and with Fe_2O_3 nanoparticles (d,e), and EDX result of the body part of a single SiNW (f), which applies to both nanowires.

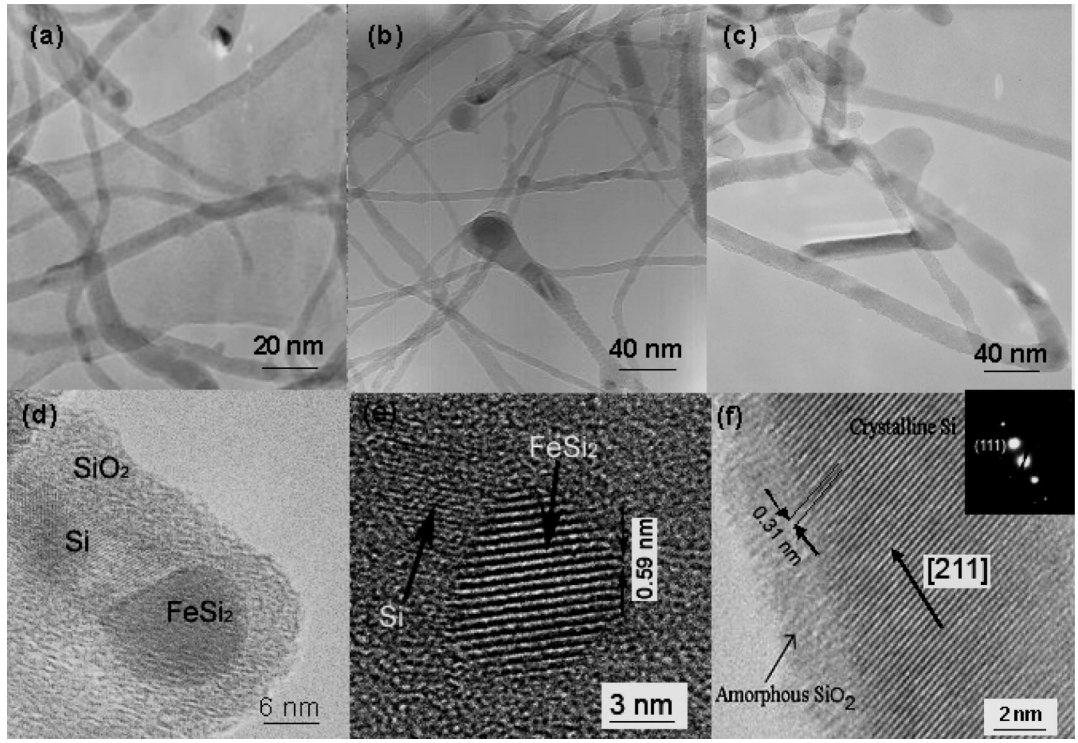

Figure 3. TEM images of SiNWs: (a) catalyzed with CNTs, (b) catalyzed with Fe_2O_3 nanoparticles, (c) HF-etched SiNWs, (d) HRTEM image of SiNW with a $FeSi_2$ catalyst, (e) lattice resolved image of the $FeSi_2$ catalyst, and (f) a SiNW.

crystalline field of the SiNWs core could influence the Si−O vibration absorption, causing the increase to a higher frequency absorption in nanowires. This phenomenon does not exist in SiO_2 nanoparticles because there is no crystalline Si core. Furthermore, certain point defects such as vacancies and broken bonds of Si−O on the interface of Si/SiO_x can also shift the strong absorption intensity to higher frequencies.[17] It is possible that the etched SiNWs promote the peaks to shift to a higher frequency because HF removed the amorphous SiO_x shell and the effects of crystalline Si became dominant.

Raman scattering is a sensitive probe to the lattice microstructure and vibrations. Phonon frequencies and scattering intensities determined by Raman spectroscopy can lead to conclusions concerning microscopic parameters such as bonding structures as well as deviation from the ideal counterpart.[18] Full profiles Raman spectra of the as-produced and the HF-etched SiNWs are shown in part b of Figure 5. The Raman shifts are positioned at 290, 504, and 929 cm^{-1} in the case of unetched SiNWs and at 279, 493, and 920 cm^{-1} for the HF-etched samples. While comparing these acquired Raman peaks of the as-prepared and the HF-etched SiNWs with the standard Raman peaks from *c*-Si (300, 520, and 930 cm^{-1}), it was observed that the peaks from pure SiNWs shifted down toward the lower frequencies and their line width became larger, as shown in part b of Figure 5. This downshift can be associated with the ultrafine feature of the SiNWs with diameters of <17 nm due to the phonon confinement.[19] In the case of fine SiNWs, more phonons appear in the Raman spectra as compared with those of *c*-Si, and the intensities of these phonons increase with decreasing the SiNWs diameter.[20,21] Therefore, the Raman peaks appeared at further lower frequencies when the SiO_x shell was etched away and the diameter of the SiNWs was further reduced.

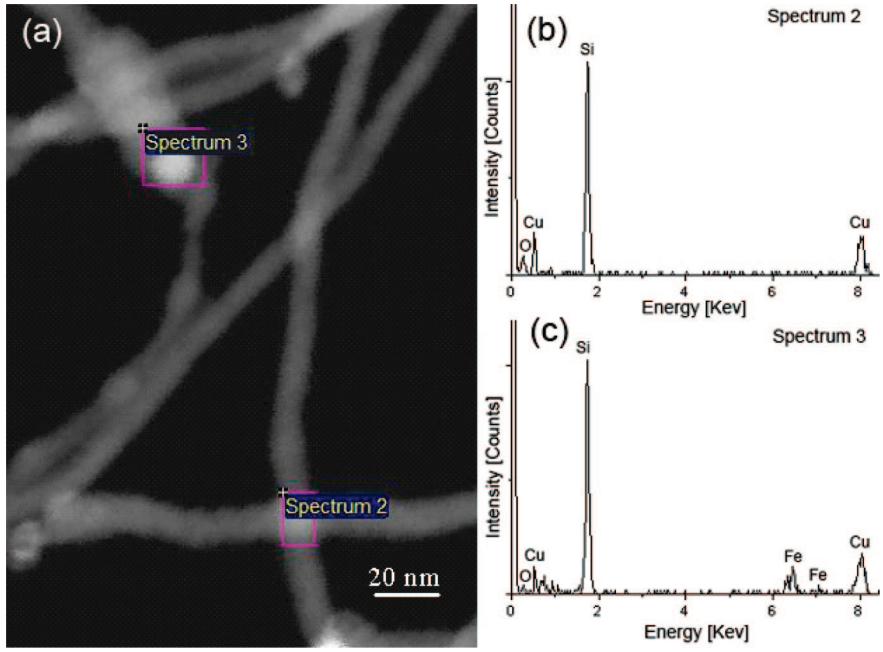

Figure 4. EDX analysis of (a) SiNWs at, (b) the wire body, and (c) the tip. The Cu signal in the spectra is from the Cu TEM grid.

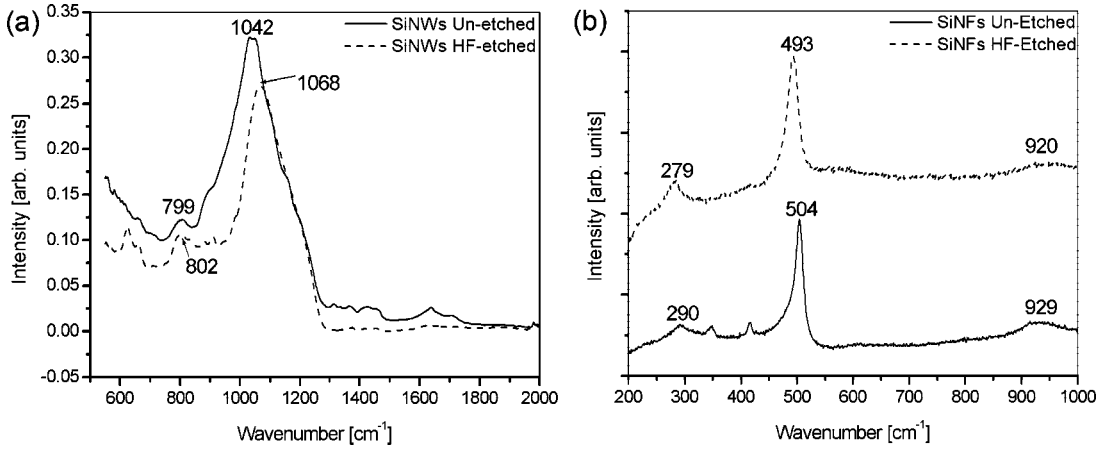

Figure 5. (a) FTIR absorption and (b) Raman spectra of the HF-etched and the as-prepared SiNWs.

Nitrogen gas-sorption measurements were employed to evaluate the effects of morphology and surface characteristics on the specific surface areas and porous features of the SiNWs. Parts a and c of Figure 6 show the N_2 adsorption/desorption isotherms of SiNWs synthesized with CNT-encapsulated Fe nanoparticles, Fe_2O_3 nanoparticles, and HF-etched nanowires. BET calculated surface areas based on the absolute adsorption are 416.71 m^2/g, 527.42 m^2/g, and 78.90 m^2/g, and pore volumes are 1.41 cm^3/g, 2.74 cm^3/g, and 0.41 cm^3/g respectively for three different samples. The desorption branches of these isotherms exhibit hysteresis as shown in parts a−c of Figure 6, corresponding to the type IV isotherm according to the IUPAC classification.[22] The existence of hysteresis loop in isotherms is due to the capillary condensation of the N_2 gas occurring in the mesopores due to the voids between particles. SiNWs have grown with the CNTs-encapsulated Fe exhibit large surface areas of ~416.73 m^2/g, which may be associated with three possible reasons: (1) ultrafine size of nanowires, (2) uniform morphology of individual nanowires forming bundles with interesting packing characteristics, and (3) the presence of oxide shell on the surface of SiNWs. Electron microscopic investigations, parts a−c of Figure 2 and part a of Figure 3, clearly illustrate that the SiNWs have ultrafine diameters <17. Further analysis, part b of Figure 9, has confirmed that the majority of nanowires have uniform morphology. Therefore, ultrafine size may contribute to the high specific areas, as already reported.[23] Existence of an amorphous SiO_x shell on the surface of the Si core is inevitable, and a close relationship between the specific surface area and surface properties of nanomaterials has already been proposed.[23] Possibly, the Si-oxide shell may be one of the leading factors responsible for the high surface area because of the porous nature of SiO_x with a high surface area (400−800 m^2/g). A thicker oxide shell offers more porous and rough surface, resulting in high surface areas due to increase in the pore volumes.[24] Further calculated specific surface areas of the etched SiNWs exhibits a drastic decrease (~81.06%), confirming the role of the surface oxide layer in the BET. HF reduces the oxide shell from the surface of SiNWs, as earlier demonstrated in part f of Figure 3, generating pure crystalline nanowires with uniform diameters, resulting in nanowire bundles with low pore volumes. A moderate ~21% increase in the calculated surface areas of SiNWs synthesized with Fe_2O_3 nanoparticles was observed, compared with those synthesized with the CNTs assistance, again shows the role of the oxide shell. This increase can be explained by the morphological characteristics of the SiNWs. Part d of Figure 2 and part b of 3 clearly show that the

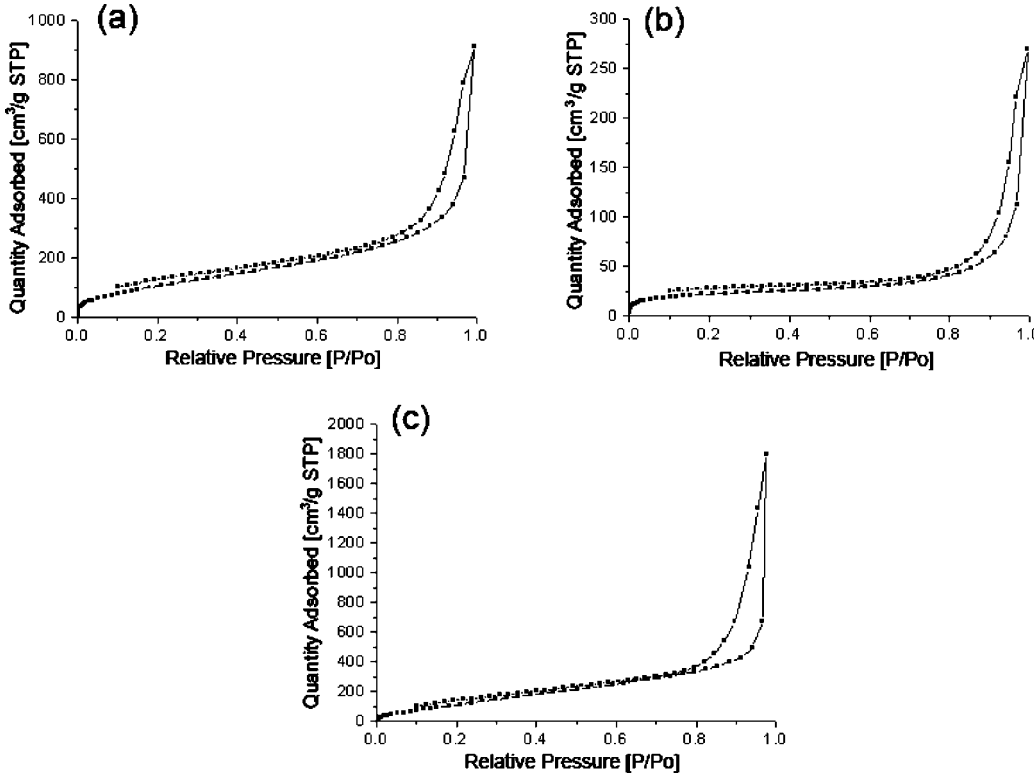

Figure 6. Nitrogen adsorption/desorption isotherms of SiNWs, (a) synthesized with CNTs, (b) HF-etched, and (c) synthesized with Fe_2O_3 nanoparticles.

nanowire bundles are composed of a combination of fine and coarse nanowires; this nonuniformity may have created extra spaces within the bundles, resulting in increased pore volumes ~48.68%.

3.3. Chemistry and Growth Mechanism. Si_3N_4 oxidizes at elevated temperature that is 1600 °C due to the presence of residue oxygen (or diffusion of oxygen from the reaction tube) in the reaction tube even though Ar flushing was applied throughout the reaction process. This phenomenon has been similarly reported during nanomaterials synthesis.[25,26] The involvement of C and Fe in the form of CNTs decreases the decomposition temperature of Si_3N_4.[27−29] The generation of SiNWs in the presence of CNTs can be explained as follows:

$$Si_3N_4 + 3O_2 \rightarrow 3SiO_2 + 2N_2 \quad (1)$$

$$2SiO_2 + C \rightarrow SiO + CO \quad (2)$$

$$2SiO \xrightarrow{Fe} Si + SiO_2 \quad (3)$$

SiO_2 is formed as a result of the oxidation of Si_3N_4 and further reduced to SiO in the presence of CNTs, which created a reducing atmosphere, as shown in eq 2. After the oxidation of CNTs, its Fe catalyst is free again to act as a catalyst for the growth of SiNWs, which formed in step 3. The presence of Fe nanoparticles at the tip of the SiNWs suggests that the SiNWs grow by following the VLS mechanism, which occurred only at temperatures >1150 °C with the Fe as catalyst.[30] The growth of SiNWs can be illustrated by a model proposed in part a of Figure 7, which represents the different temperature zones that are responsible for the nucleation and growth of the SiNWs. CNTs in the precursor mixture are oxidized at low temperature at 500−600 °C and left behind clusters of Fe catalyst. In zone-I, temperatures between 1400−1600 °C, vapors of Si and Fe are rapidly condensed into a Si-rich liquid cluster. When the

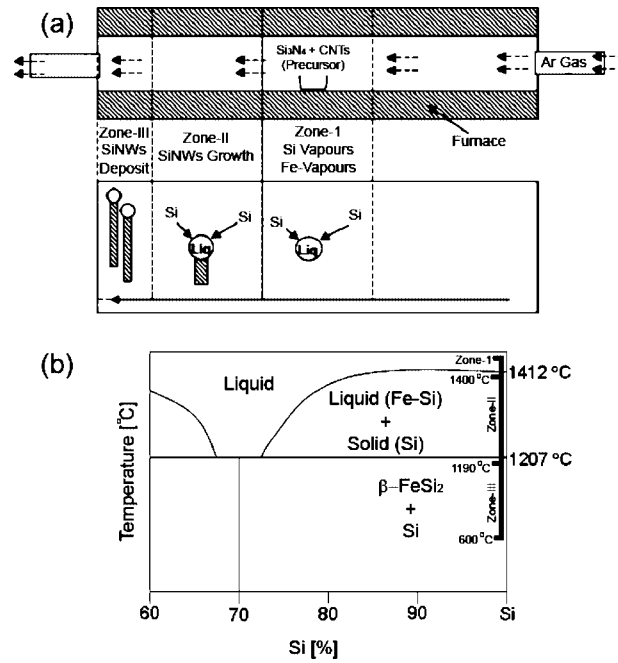

Figure 7. (a) Growth mechanism for the SiNWs, (b) Si−Fe phase diagram.

cluster becomes supersaturated, the Si phase precipitates and crystallizes in the form of a nanowire. The growth terminates automatically when the gas flow carries nanowires out of zone-II, temperatures in the range of 1190−1400 °C, and finally a thick film of SiNWs deposits at low temperature zone-III (<600 °C). According to the Si−Fe phase diagram, part b of Figure 7, the terminating solid clusters are $FeSi_2$. $FeSi_2$ is a stable Fe−Si compound in the Si-rich region, and it is believed that the nanowires growth terminates at below 1207 °C because no liquid exists below that temperature. Quantitative EDX analysis of the

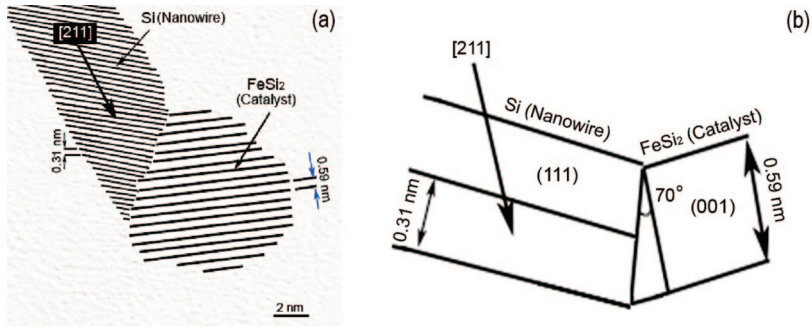

Figure 8. Schematic model of (a) SiNWs growth and (b) SiNW−$FeSi_2$ interface.

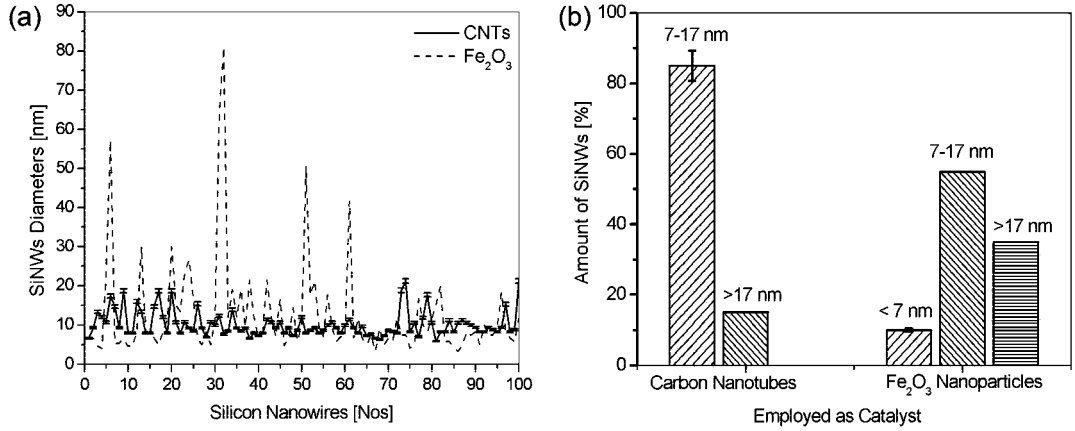

Figure 9. Diametric (a) distribution and (b) uniformity analysis of SiNWs synthesized with CNTs and Fe_2O_3 nanoparticles.

nanowires tip shows, part c of Figure 4, that the Fe−Si clusters have the expected $FeSi_2$ composition, whereas measurements made away from the tip detected no Fe, as seen in part b of Figure 4.

On the basis of the HRTEM image of the interface of catalyst and nanowire shown in part e of Figure 3, a schematic model can be developed to explain the structural features, as displayed in part a of Figure 8. The atomic planes of the catalyst phase are separated by 0.59 nm, enlarged slightly (∼13%) compared with the fringe separation recorded in previous studies that is 0.51 nm,[31] corresponding to the fringe separation of the (001) planes in $FeSi_2$. The SiNW exhibits fringe separation of 0.31 nm agreeing with the (111) planes. A close inspection of the interface model in part b of Figure 8 has revealed that Si (111) planes are oriented at an angle of ∼70° to the growth direction, which is nearly 17−20° off the axis of (111) plane. This strongly suggests a [211] growth because the [211] and [111] directions are 19.47° apart,[32] as confirmed by the SAED investigation shown in part f of Figure 3. Previous studies have revealed that the growth direction of SiNWs using Fe-catalytic was generally along [111], and partially along [211]; however, the growth direction is diameter dependent. SiNWs larger than ∅ 20 nm generally grow along the [111] direction, and with smaller diameters of a few nanometers the [211] growth direction is preferable.[33]

The crystallographic lattice structure at the interface is important for defining the structural characteristics of the nanowires. During VLS growth, the interface between the catalyst and the nanowire prefers to take the least lattice mismatch and requires a reasonable value to promote the epitaxial growth. In the present case, the lattice mismatch between $FeSi_2$ (001) and Si (111) planes is ∼5.08%, which agrees well with the epitaxial growth requirements, as shown in part b of Figure 8. In connection to the crystalline plane mismatch between the catalyst and SiNWs, studies on the growth of SiC nanowires using Fe−Co catalyst have shown that the Fe-based combination slightly altered the *d*-spacing of the catalyst and then matched by proper SiC planes.[34] It is likely that by choosing the metal catalyst with a specific *d*-spacing, it is possible to control the growth direction of SiNWs. Thus, it is believed that the interface between Si crystal and $FeSi_2$ nanoclusture may favor the growth of high-density and low-energy Si (111) planes. A specific plane of $FeSi_2$, for example (001), may have significant role in initiating the nucleation and subsequent growth of Si (111) planes in a particular orientation, resulting in controlled morphology and orientation.[35] The alteration of $FeSi_2$ *d*-spacing has not yet been reported in previous studies using Fe to catalyze the growth of SiNWs; however, understanding the phenomenon needs further investigation.

3.4. Dimensional Analysis. Analysis of images taken from a number of SiNWs grown under similar conditions has showed that the diameters of SiNWs synthesized with the assistance of CNTs are much more uniform as compared to those synthesized with Fe_2O_3 nanoparticles, as illustrated in part a of Figure 9. Part b of Figure 9 exhibits that more than 85% SiNWs have diameters between 7 and 17 nm and less than 15% have diameters >17 nm, when CNTs were employed. By using Fe_2O_3 nanoparticles, a wide difference in diameters was observed, as 10% <7 nm, 55% between 7 and 17 nm, and 35% >17 nm. It is believed that CNTs facilitate the pyrolysis of Si_3N_4 because carbon reduces the reaction temperatures via forming a nanostructure in the carbothermal reduction process and assists in the subsequent growth of SiNWs by donating its Fe catalyst. The size of the SiNWs depends on the sizes of the catalyst provided during a VLS growth. CNTs have a vital role in producing uniform and even diameter nanowires because the size of the Fe catalyst is confined by the size of the CNTs. In

addition, Fe-catalysts are encapsulated within carbon multilayers and have no interaction with each other; hence, it is believed that the chances of Fe agglomerating to form clusters are almost negligible. Another advantage of CNTs is that it always keeps Fe nanoparticles in an active state and maintains a highly activated reducing atmosphere when Si diffused into them.[14] In the other case, Fe_2O_3 nanoparticles are always present in the form of uneven clusters with wide differences in diameter and it is also difficult to maintain a minimum and uniform diameter. Hence, the size confinement effect is not present in this case, consequently resulting in SiNWs having diameters with severe variation.

4. Conclusions

Ultrafine SiNWs, <17 nm, have been successful generated in high yield with the assistance of CNTs. Eighty-five percent of as-produced nanowires have diameters between 7 and 17 nm, as compared to the SiNWs produced at a similar conditions using Fe_2O_3 nanoparticles as the catalyst, which have larger diameter differences and only 55% have diameters between 7 and 17 nm. TEM study has confirmed that the SiNWs have a single-crystalline Si core and a tiny amorphous shell of SiO_x. The presence of Fe nanoparticles at the tip of SiNW suggests that the growth of SiNWs follows the VLS mechanism. During the SiNWs synthesis process, CNTs assisted in two ways, one by facilitating the pyrolysis of Si_3N_4 by carbothermal reduction and therefore by donating its Fe catalyst to again act as a catalyst for SiNWs growth along the [211]; hence, the SiNWs are uniform in diameter as compared to those synthesized with Fe_2O_3 nanoparticles. Combined HRTEM characterizations have shown that the ultrafine SiNWs have a corresponding growth plan against the $FeSi_2$ catalyst phase. The ultrafine SiNWs can be further reduced in diameter by etching away the oxide shell. These SiNWs exhibit large BET specific surface areas ~416.71 m^2/g, which could be very useful in catalyst or fuel-cell applications.

Acknowledgment. I.A. wishes to thank the Government of Pakistan and School of Mechanical, Materials and Manufacturing Engineering, The University of Nottingham, United Kingdom for support his study. Y.Q. thanks Keith Dinsdale and Thomas Buss for their technical support.

References and Notes

(1) Iijima, S. *Nature* **1991**, 354.
(2) Zhu, Y. Q.; Hu, W. B.; Hsu, W. K.; Kroto, H. W.; Walton, D. R. M. *Adv. Mat.* **1999**, *11*, 844.
(3) Buttner, C. C.; Zacharias, M. *Appl. Phys. Lett.* **2006**, 89.
(4) Wang, N.; Tang, Y. H.; Zhang, Y. F.; Lee, C. S.; Lee, S. T. *Phys. Rev.* **1998**, B 58.
(5) Bootsma, G. A.; Gassen, H. J. *J. Cryst. Growth* **1971**, 223.
(6) Wang, N.; Tang, Y. H.; Zhang, Y. F.; Lee, C. S.; Bello, I.; Lee, S. T. *Chem. Phys. Lett.* **1999**, 237.
(7) Westwater, J.; Gosian, D. P.; Tomiya, S.; Usui, S.; Ruda, H. *J. Vac. Sci. Technol.* **1997**, *B15*, 54.
(8) Ozaki, N.; Ohno, Y.; Takeda, S. *Appl. Phys. Lett.* **1998**, *73*, 3700.
(9) Sunkara, M. K.; Sharma, S.; Miranda, R.; Lian, G.; Dickey, E. C. *Appl. Phys. Lett.* **2001**, *79*, 1546.
(10) Zhao, X. T.; Hu, J. Q.; Li, C. P.; Ma, D. D. *Chem. Phys. Lett.* **2003**, *369*, 220.
(11) Wagner, R. S.; Ellis, W. C. *Appl. Phys. Lett.* **1964**, *4*, 89.
(12) *Whisker Technology*, Wagner, R. S.; Levitt, A. P., Eds.; *Willey-Interscience*: New York, 1970; 47.
(13) Trentler, T. J. *Science* **1995**, 1791.
(14) Li, C.; Gu, C.; Yang, Y. *Chem. Phys. Lett.* **2005**, 198.
(15) Gundiah, G.; Deepak, F. L.; Govindaraj, A. C.; Rao, N. R. *Chem. Phys. Lett.* **2003**, 579.
(16) Kirk, C. T. *Phys. Rev.* **1998**, *B 38*, 1255.
(17) Hu, Q.; Suzuki, H.; Gao, H.; Nado, T. *Chem. Phys. Lett.* **2003**, *278*, 299.
(18) Zhang, S. L. *App. Phys. Lett.* **2002**, 44.
(19) Wang, R. P.; Zhou, G. W.; Zhang, Z. *Phys. Rev.* **2000**, 827.
(20) Li, C.; Gu, C.; Mi, J.; Yang, Y. *Chem. Phys. Lett.* **2005**, *411*, 198.
(21) Eklund, P. C. *Proc. of the XVIIIth. Int. Conf. Raman Spectr.*, Willey, New York, 2002.
(22) Sing, K. S. W.; Everett, D. H.; Pierotti, R. A.; Siemieniewska, T. *Pure Appl. Chem.* **1985**, *57*, 603.
(23) Zhao, Y. M.; Hu, W. B.; Gregory, D. H.; Zhu, Y. Q. *J. Mater. Chem.* **2007**, *17*, 4436.
(24) Wang, Y.; Shen, J. *Mater. Lett.* **1983**, *72*, 36.
(25) Morless, M. A.; Lieber, C. M. *Science* **1998**, *279*, 208–210.
(26) Kim, H. N.; Kim, W. H. *Appl. Surf. Sci.* **2005**, *242*, 29–34.
(27) Pasto, E. *J. Am. Ceram. Soc.* **1984**, *67*, 178.
(28) Zhou, F.; Suh, C.; Kim, S. S. *Mater. Lett.* **2002**, *55*, 55.
(29) Cao, G.; Hwang, Z. K.; Fu, X. R. *Chin. Sci.* **1985**, *A4*, 379.
(30) Hu, J.; Wang, T.; Lieber, C. M. *Acc. Chem. Res.* **1999**, *32*, 435.
(31) Alfredo, M.; Lieber, C. M. *Science* **1998**, *279*, 208.
(32) Barsotti, R. J.; Fischer, J. E.; Mohd., J. *Appl. Phys. Lett.* **2002**, *81*, 2866.
(33) Zhang, Z. Y.; Siu, G. G. *J. Cryst. Growth* **2005**, *285*, 620.
(34) Zhu, Y. Q.; Hu, W. B.; Kroto, H. W.; Terrones, H. *J. Mater. Chem.* **1999**, *9*, 3173.
(35) Tan, T. Y.; Lee, S. T. *Appl. Phys. Mater. Sci. Proc.* **2002**, *74*, 423.

JP808492T